Solution Structure of Pyoverdin GM-II†

Gerold Mohn,* Patrice Koehl,‡ Herbert Budzikiewicz,§ and Jean-François Lefèvre‡

Centre National de la Recherche Scientifique, Institut de Biologie Moleculaire et Cellulaire, 15 rue René Descartes, F-67084 Strasbourg, France, and Institut für Organische Chemie der Universität Köln, Greinstrasse 4, D-50939 Köln, Germany

Received September 30, 1993; Revised Manuscript Received December 14, 1993•

ABSTRACT: The three-dimensional structure in solution of ferri-pyoverdin GM-II isolated from the culture medium of *Pseudomonas fluorescens* was determined by application of NMR methods to the Ga^{3+} analogue. Distance geometry calculations were performed with FILMAN using interproton distances and coupling constants as constraints. Further conformational analysis was carried out by energy minimization with MM2 and AMBER. Back-calculation of the NOESY spectra shows that the resulting structures are in agreement with the experimental data.

Iron is a trace element essential for the redox systems in nearly all organisms. Under aerobic conditions its most stable oxidation state is Fe(III), whose oxide hydrates are poorly soluble in water at physiological pH values ($K_L = 10^{-38}$ at pH 7). In order to overcome iron deficiency, many bacteria and fungi have developed highly specific iron acquisition systems. Most of them are based on complexation of the available Fe(III) by strong chelators called siderophores. Usually microorganisms recognize only their own siderophore by outer membrane proteins.

Pseudomonas spp. of the so-called fluorescent group, to which belongs inter alia the human pathogenic *Pseudomonas aeruginosa*, produce peptidic siderophores named pyoverdins when grown in an iron-deficient medium. Their common feature is the chromophore (1*S*)-5-amino-2,3-dihydroxy-1*H*-pyrimido[1,2-*a*]quinoline-1-carboxylic acid. Its 5-amino group is linked to a dicarboxylic acid belonging to the citric acid cycle while the 1-carboxyl group is bound in most cases to the N-terminus of a linear or cyclic peptide containing 6–12 amino acids (Budzikiewicz, 1993). Cross-feeding experiments have shown that usually a given *Pseudomonas* strain accepts only its own pyoverdin. Strain specificity for pyoverdin-mediated iron uptake was systematically investigated for *P. aeruginosa*, *P. fluorescens*, *P. putida*, *P. chlororaphis*, and *P. tolasii* by cross-feeding, iron-uptake studies, and binding experiments (Hohnadel & Meyer, 1988; Cornelis et al., 1989). However, nothing is known about the nature of the amino acids and the steric requirements for the interaction of a pyoverdin with the cell surface proteins. We intend, therefore, to investigate the strain specificity on the basis of the three-dimensional molecular structure of the pyoverdin complexes in solution as derived from NMR[1] spectroscopic data. So far it is only known that Fe(III) forms octahedral complexes and thus provides six coordination sites which can accommodate three bidentate ligands. The catecholic moiety of the chromophore is one of the complexing groups. The other two (α-hydroxycarboxylic or hydroxamic acids) are located in the peptide residue.

Recently, the primary structure of pyoverdins GM-I and GM-II (Figure 1) was elucidated (Mohn et al.,1990). In this paper we describe the determination of the three-dimensional structure of the Ga(III) complex of pyoverdin GM-II by NMR spectroscopic studies, distance geometry calculation, and restrained molecular mechanics.

EXPERIMENTAL PROCEDURES

CD Spectroscopy of Ferri-GM-II. CD spectra were recorded on a Dichrograph Mark III (ISA) in buffered aqueous solution (0.1 N Tris·HCl, pH 7.2).

Preparation of the Ga(III) Complex. Ferri-GM-II (40 mg) was dissolved in 3 mL of 0.1 N acetic acid, and, after adjusting the pH to 3.0 with diluted aqueous NH_3, 100 mg of gallium-(III) nitrate and 300 mg of ascorbic acid in 3 mL of 0.1 N acetic acid were added. After the pH of the solution was adjusted to 5.0, the Ga(III) complex was adsorbed on XAD-4 resin, washed with water, and desorbed with acetonitrile/water (1:1, v/v). The extract was purified by chromatography on Bio-Gel P-2 with a 0.1 M pyridinium acetate buffer (pH 6.5); the yield was 32 mg. The purity of the Ga complex was demonstrated by RP-HPLC on Polygosil 60-C18, eluted with 5% acetonitrile in 0.1 M ammonium acetate buffer (pH 6.2). In the PI-FAB mass spectrum the masses of the $[M+H]^+$ ions of the free ligand and the Ga(III) complex differ by 66 amu ($+^{69}Ga - 3H$) and 68 amu ($+^{71}Ga - 3H$).

NMR Spectroscopy. NMR experiments were performed on a Bruker AMX 500 spectrometer. Data processing was achieved with an Aspect X32 computer using UXNMR software or with FELIX (Biosym) running on Indigo (Silicon Graphics). The measurements were performed with 10 mM solutions of Ga pyoverdin GM-II or of the free ligand in CD_3COONa/CD_3COOH buffered H_2O/D_2O 95/5 (v/v) in a pH range between 2.0 and 6.5 and in a temperature range between 278 and 313 K. The water resonance was suppressed using the jump-and-return method (Plateau & Guéron, 1982) or by presaturation during the relaxation delay. COSY, RE-

† This work was supported by a Merrell/Dow-Université Louis Pasteur Fellowship of the Académie des Sciences.

* To whom correspondence should be addressed. Present address: Bayer AG Wuppertal, Geb. 302, Friedrich-Ebert-Strasse, D-42117 Wuppertal, Germany.

‡ CNRS.

§ Institut für Organische Chemie der Universität Köln.

• Abstract published in *Advance ACS Abstracts*, February 15, 1994.

[1] Abbreviations: CD, circular dichroism; Chr, chromophore; *d*, distance (Å); COSY, correlated spectroscopy; DSS, 3-(trimethylsilyl)-1-propanesulfonic acid; FAB-MS, fast atom bombardment mass spectrometry (PI = positive ion); HOHAHA, homonuclear Hartmann–Hahn spectroscopy; (OH)Asp, *threo*-3-hydroxyaspartic acid; NMR, nuclear magnetic resonance; NOE, nuclear Overhauser enhancement; NOESY, nuclear Overhauser enhancement spectroscopy; (OH)Orn, N^5-hydroxyornithine; rmsd, root mean square deviation; RP-HPLC, reversed-phase high-performance liquid chromatography; SD, standard deviation of atomic positions; Suc, succinic acid.

0006-2960/94/0433-2843$04.50/0

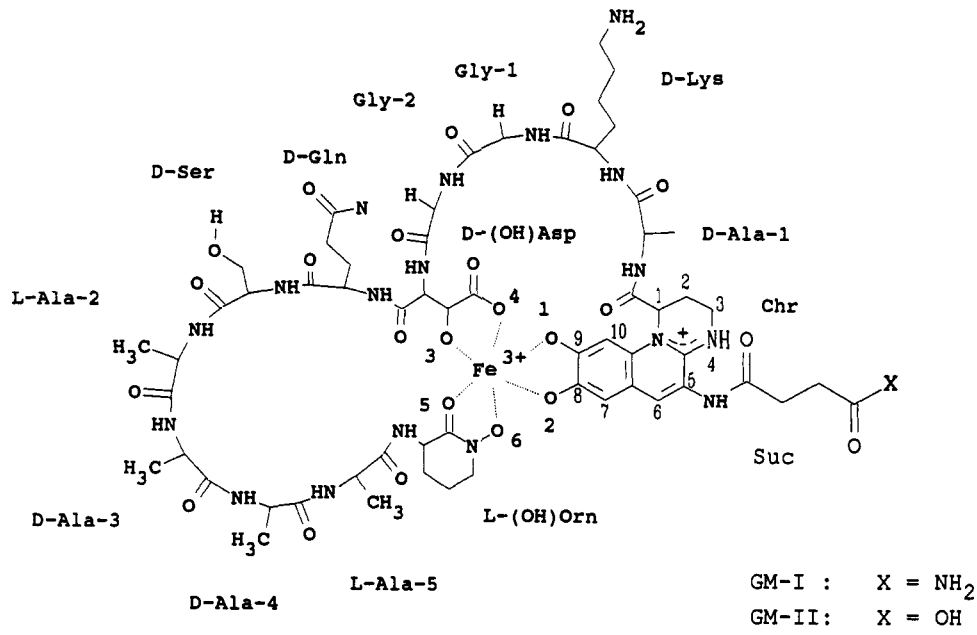

FIGURE 1: Structure of the ferri-pyoverdins GM-I and GM-II.

LAYED COSY, and MLEV17 HOHAHA data were acquired in the phase-sensitive mode using the time-proportional phase incrementation scheme (TPPI) (Marion & Wüthrich, 1983). The spectral width in F_1 and F_2 was 5435 Hz. A total of 512 experiments with 8 or 16 scans of 1024 complex data points in t_2 were collected. NOESY spectra were performed with the States phase incrementation scheme (States et al., 1982). A total of 1024 experiments with 2048 complex data points were recorded. In HOHAHA experiments the mixing time was 40 ms. NOESY spectra were acquired with mixing times between 50 and 500 ms. The time domain data were zero filled in F_1. Resolution enhancement was obtained by apodization of the time domain data with a $\pi/3$-shifted squared sine bell. H/D exchange rates were measured by dissolving a Ga complex sample lyophilized from a H_2O solution in CD_3COONa/CD_3COOH buffered D_2O (pH 4.5) and following the decrease of the ^1H resonances by repeated measurement of one-dimensional ^1H NMR spectra. The exchange rates were calculated as the first-order rate constants of the decrease of magnetization.

NOE Measurements. Interproton distances were calculated from the cross peak volumes in the NOESY spectrum under the rigid body approximation, i.e., a single correlation time τ_c was assumed for all interacting vectors. The interproton distances d_{ij} were calculated using (Wüthrich, 1986):

$$d_{ij} = d_{cal}(NOE_{cal}/NOE_{ij})^{1/6}$$

where d_{cal} is a known distance between two protons used for calibration and NOE_{cal} is the corresponding cross peak volume. As reference we used the distance between the amide proton and Hα of (OH)Orn calculated from the coupling constant $^3J_{NH-H\alpha}$ according to the Karplus relationship (Karplus, 1959). This distance was found to be 2.95 Å. Ten intraresidue, 16 sequential, and 7 long-range distance constraints were used for further calculations.

Distance Geometry Calculations with FILMAN. FILMAN calculations (Koehl et al., 1992) were performed on an IBM RS6000 system or on a personal computer with a 80486 processor. Since FILMAN was designed for proteins with standard amino acids, several modifications were necessary in order to treat the Ga complex.

The chromophore was constructed using bond distances and angles taken from the crystal structure of pseudobactin (Teintze et al., 1981). The aliphatic part (dihydropyrimidine ring, Figure 1) was kept planar during all FILMAN calculations because the accuracy of our distance constraints was not sufficient to determine the exact conformation of the ring. Ga^{3+} was fixed to the catecholic oxygens. Coordination of the two other ligands was implied by distance constraints. The (OH)Orn cyclus was also kept planar with bond distances corresponding to those of pseudobactin.

Concerning the methylene protons of the glycine residues, no information about their stereospecific assignment was available. Therefore the two methylene protons were replaced by a pseudoatom between the original protons. Distance constraints were increased accordingly by 1 Å.

Starting structures were constructed by random generation of the dihedral angle set. For all dihedral angles an initial variance of 90° was applied. Each structure was refined in 30 iteration steps. After each iteration, the quality of the estimated structure was evaluated on the basis of the average and maximum errors as well as the χ^2 value (Koehl et al., 1992), which is defined by:

$$\chi^2 = \sum[(d_{exp} - d_{calc})/\text{error}]^2 + \sum[(J_{exp} - J_{calc})/\text{error}]^2$$

The refined structures were stored when the resulting average error was lower than 1.5 Å and the maximum error lower than 5 Å. All resulting structures were further optimized in 30 iteration steps with a variance of 10° for the dihedral angles. The structure with the lowest average error was stored for further investigation.

Energy Minimization. Energy minimization was performed on a personal computer with the MM+ routine of the HYPERCHEM software (Autodesk). MM+ is an implementation of Allingers MM2 force field (Allinger, 1977). Chr, (OH)Asp, and (OH)Orn were incorporated in the template files. The published parameter set was modified for the coordination sphere using a bond dipole moment of 2.5 Debye, a minimum bond length of 2.0 Å, and a stretching force constant of 180 kcal/mol·Å^2 for the Ga^{3+}–O bond. Interproton distances and hydrogen bonds were constrained with force constants of 25 kcal/mol allowing deviations up to

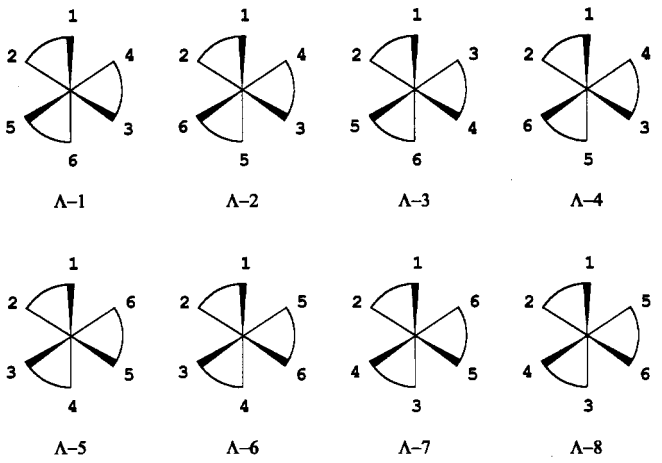

FIGURE 2: Eight possible Λ-isomers of ferri-pyoverdin GM-II. The corresponding Δ-isomers are the mirror images.

0.3 Å. This is in accordance with the estimation errors of our NOE derived distances. Energy minimizations were performed using the block diagonal Newton Raphson method (Fletcher, 1980; Gill et al., 1981). Most of the calculations converged to an energy descent of 0.1 kcal/mol per iteration step.

Further refinement was achieved with the AMBER force field (Weiner et al., 1984; Weiner et al., 1986) using the AMBER 3.0 parameter set. The partial charges of the chelating oxygens were set to –0.4 and for the Ga to +0.5 as calculated semiempirically with PM3 (Stewart, 1989a,b). Partial charges of the other atoms were calculated with MNDO (Stewart, 1990). The values for the standard amino acids correlated well with the charges given in the AMBER 3.0 parameter set. Optimization was performed using the Polak–Ribiere conjugate gradient method (Fletcher, 1980; Gill et al., 1981). The convergence limit was 0.01 kcal/mol per iteration step.

NOE Back-Calculation. We used NOE back-calculation as an additional check for the quality of our set of final structures. This approach (Banks et al., 1989) consists of building a theoretical NOE spectrum from the coordinates of each proton in the molecule and a model for its dynamics. Calculations were performed using the program STATICNOE (Koehl, unpublished).

RESULTS

CD Spectroscopy

The solution structure of pyoverdins is characterized by two features, i.e., the absolute configuration of the coordination sphere and the conformation of the peptide chain. In order to determine the absolute configuration, 16 different sterical arrangements, eight Δ- and eight Λ-configurations, have to be considered. The Λ-configurations are shown in Figure 2. For many pyoverdins the major portion of the configurations can be excluded because of steric hindrance by simply examining a CPK model. However, all 16 configurations have to be considered for ferri-pyoverdin GM-II, because this molecule has a longer and more flexible peptide chain as compared with other pyoverdins. The absolute configuration (Δ or Λ) of siderophores can be determined by CD spectroscopy.

The siderophore triacetylfusarinine was isolated in two different diasteromeric crystalline forms (Λ-*cis* and Δ-*cis*) by crystallization from different solvents (Hossain et al., 1980).

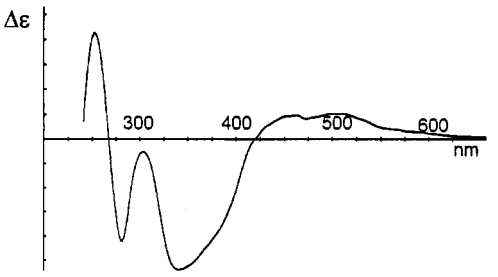

FIGURE 3: CD spectrum of ferri-pyoverdin GM-II in buffered aqueous solution (0.1 N Tris·HCl, pH 7.2).

The absolute configuration was determined by anomalous X-ray dispersion.

The CD spectrum of the Λ-*cis* crystals (in KBr disc) shows a strong positive Cotton effect in the region of the ligand-to-metal charge transfer bands ($\Delta\epsilon = -5$ at 370 nm, $\Delta\epsilon = 0.8$ at 500 nm). The CD spectrum of the Δ-*cis* form is the exact mirror image. In solution the CD bands are qualitatively similar to those of the Λ-*cis* isomer, and therefore it was concluded that triacetylfusarinine is predominantly Λ-*cis* configured in solution (Hossain et al., 1980).

The CD spectra of pyoverdines show a Cotton effect between 400 and 600 nm derived from the ligand-to-metal charge transfer absorptions between 470 and 550 nm. The Cotton effect caused by the strong chromophore absorption at 400 nm occurs between 300 and 500 nm. The chromophore is *S*-configured in all known pyoverdins, but the Cotton effect is highly influenced by the nature of the peptidic part as shown by investigation of several pyoverdins (G. Mohn, unpublished).

In crystalline form, ferri-pseudobactin (Teintze et al., 1981) is Λ-configured. Its CD bands at 436 (–0.8) and 502 (0.3) nm ($\Delta\epsilon$) caused by the charge transfer absorption are qualitatively similar to those of triacetylfusarinine C. However, the intensity of the Cotton effect is about one order of magnitude lower than that of ferrichrome. Therefore, one cannot exclude an equilibrium of Λ- and Δ-isomers.

In the spectrum of ferri-pyoverdin GM-II (Figure 3) the CD bands of the coordination center are partially superimposed by the chromophore bands. However, the spectrum shows a positive $\Delta\epsilon$ in the whole range above 500 nm ($\Delta\epsilon = 1.4$ at 505 nm). Therefore we concluded that the iron complex of pyoverdin GM-II is mainly Λ-configured in solution especially as the intensity of the CD band is comparable to that of ferrichrome.

NMR Spectroscopy

(a) Assignment of Resonances. A partial assignment of the ^{1}H NMR resonances of the free ligand was published in a previous paper (Mohn et al., 1990).

The Fe(III) complex is paramagnetic and cannot be studied by NMR spectroscopy. The diamagnetic Ga(III) analogues are known to be suitable isomorphous model systems for NMR-spectroscopic investigations of siderophores (van der Helm et al., 1981; Constantine et al., 1990). Gallium-pyoverdin GM-II was prepared and purified as described above. The ^{1}H chemical shifts are given in Table 1. The spin systems of the amino acids, succinic acid, and the aliphatic part of the chromophore were identified by ^{1}H-COSY, RELAYED COSY, and HOHAHA experiments. The assignment of the aromatic chromophore protons was confirmed by NOESY cross peaks between H-10 and H-1 as well as H-6 and H-7. NH protons of the chromophore were identified by the NOESY cross peaks H6/NH5 and NH5/H4. Sequential assignments are based on NH_i–NH_{i+1}, $C\alpha H_i$–NH_{i+1} and

Table 1: ^{1}H Chemical Shifts of Pyoverdin GM-II and Its Ga(III) Complex[a]

proton	δ(GMII)	δ($GMII_{Ga}$)	Δδ[b]
Suc-H2′	2.77	2.70	−0.07
Suc-H3′	2.73	2.68	−0.05
Chr-NH5	9.96	9.55	−0.41
Chr-H1	5.59	5.60	0.01
Chr-H2a	2.48	2.34	−0.14
Chr-H2b	2.70	2.64	−0.06
Chr-H3a	3.39	3.20	−0.19
Chr-H3b	3.72	3.58	−0.14
Chr-H4	8.86	8.11	−0.75
Chr-H6	7.91	7.72	−0.19
Chr-H7	7.11	6.68	−0.43
Chr-H10	6.98	7.07	0.09
Ala^1-NH	9.47	9.15	−0.32
Ala^1-Hα	4.41	4.36	−0.05
Ala^1-Hβ	1.49	1.39	−0.10
Lys-NH	8.64	8.44	−0.20
Lys-Hα	4.25	4.02	−0.23
Lys-Hβ	1.64/1.79	1.66/1.71	0.02/−0.08
Lys-Hγ	1.20	1.28/1.40	−0.08/0.20
Lys-Hδ	1.46	1.59	0.13
Lys-Hε	2.68	2.89	0.21
Lys-εNH	7.47	7.45	−0.02
Gly^1-HN	8.47	9.37	−1.10
Gly^1-Hα	3.92	3.98	0.06
Gly^2-NH	8.37	9.13	0.76
Gly^2-Hα	3.95/4.12	3.75/4.15	−0.20/0.03
(OH)Asp-NH	8.34	9.02	0.68
(OH)Asp-Hα	4.81	4.19	−0.62
(OH)Asp-Hβ	4.57	4.35	−0.22
Gln-αNH	8.58	6.69	−1.89
Gln-Hα	4.39	3.98	−0.41
Gln-Hβ	1.87/2.00	1.09/1.24	−0.78/0.76
Gln-Hγ	2.34	1.69	−0.65
Gln-NH2	6.95/7.62	7.02/7.84	0.07/0.22
Ser-NH	8.43	10.14	1.71
Ser-Hα	4.42	4.14	−0.28
Ser-Hβ	3.89	3.80/4.14	−0.09/0.25
Ala^2-NH	8.42	7.30	−1.12
Ala^2-Hα	4.33	4.14	−0.19
Ala^2-Hβ	1.43	1.36	−0.07
Ala^3-NH	8.31	8.89	0.58
Ala^3-Hα	4.29	3.95	−0.34
Ala^3-Hβ	1.39	1.39	0.00
Ala^4-NH	8.43	7.83	−0.60
Ala^4-Hα	4.29	4.06	−0.23
Ala^4-Hβ	1.43	1.45	0.02
Ala^5-NH	8.43	7.01	−1.42
Ala^5-Hα	4.25	4.15	−0.10
Ala^5-Hβ	1.43	1.26	−0.17
(OH)Orn-NH	8.45	7.77	−0.68
(OH)Orn-Hα	4.44	4.70	0.26
(OH)Orn-Hβ	1.87/2.03	1.76/2.11	−0.11/0.08
(OH)Orn-Hγ	2.03	1.94/2.03	−0.09/0.00
(OH)Orn-Hδ	3.63/3.68	3.49/3.57	−0.14/−0.11

[a] ppm relative to DSS, buffered H_2O/D_2O (95/5, v/v), pH 5.0, 278 K. [b] δΔ = δ($GMII_{Ga}$) − δ(GMII).

$C\beta H_i$–NH_{i+1} NOEs. Figure 5 shows the region of the NH/Hα cross peaks in the NOESY spectrum.

The large conformational changes induced by metal binding as compared with the free ligand can be seen from the displacement of resonances especially in the NH range (Table 1). The broad chemical shift distribution in the NH region indicates strongly restricted dynamics due to the conformational stabilization of the complex. The proton chemical shifts are highly influenced by the shielding and deshielding effects of the aromatic part of the chromophore.

For the NH protons of the Ga complex, a linear temperature dependence of the chemical shifts was observed between 278 and 313 K (data not shown) while for the free ligand a linear behavior occurred only below 298 K, indicating an important structural change. From the weak temperature dependance of the chemical shifts and the retarded H/D exchange rates, we conclude that in the Ga complex the NH protons of Gly^2 ($\Delta\delta/\Delta T = 1.38 \times 10^{-3}$ ppm/K, $t_{1/2}$ = 320 min), (OH)Asp ($\Delta\delta/\Delta T = 1.33 \times 10^{-3}$ ppm/K, $t_{1/2}$ = 420 min), Ser ($\Delta\delta/\Delta T$

Table 2: Distance Constraints for FILMAN Calculations and Energy Minimization[a]

atom 1	atom 2	distance (Å)	FILMAN variance (Å)
	Coordination Constraints[b]		
Ga	(OH)Asp-Oβ	2.00	0.02
Ga	(OH)Asp-Oγ1	2.00	0.02
Ga	(OH)Asp-Cβ	2.87	0.02
Ga	(OH)Asp-Cγ	2.82	0.02
Ga	(OH)Orn-O	2.00	0.02
Ga	(OH)Orn-Oδ	2.00	0.02
Ga	(OH)Orn-C	2.79	0.02
Ga	(OH)Orn-Nδ	2.80	0.02
	Additional Constraints for Λ-2[b]		
Chr-O1	(OH)Asp-Oβ	3.00	0.05
Chr-O1	(OH)Asp-Oγ1	3.00	0.05
Chr-O1	(OH)Orn-O	3.90	0.05
Chr-O1	(OH)Orn-Oδ	3.00	0.05
Chr-O2	(OH)Asp-Oβ	3.90	0.05
Chr-O2	(OH)Asp-Oγ1	3.00	0.05
Chr-O2	(OH)Orn-O	3.00	0.05
Chr-O2	(OH)Orn-Oδ	3.00	0.05
(OH)Asp-Oβ	(OH)Orn-O	3.00	0.05
(OH)Asp-Oβ	(OH)Orn-Oδ	3.00	0.05
(OH)Asp-Oγ1	(OH)Orn-O	3.00	0.05
(OH)Asp-Oγ1	(OH)Orn-Oδ	3.00	0.05
	Hydrogen Bond Constraints		
Gly^2-HN	Ala1-O	2.00	0.10
Gly^2-N	Ala^1-C[b]	4.50	0.10
Ala^5-HN	Ala^2-O	2.00	0.10
Ala^5-N	Ala^2-C[b]	4.50	0.10

[a] The 33 interproton distances derived from NOESY spectra are not shown. The FILMAN variance was always 5% of the calculated distance. For energy minimization a force constant of 25 kcal/mol was applied. [b] These constraints were only applied in FILMAN calculations.

Table 3: Configuration of the FILMAN Structures

structure	configuration-type	refinement step 1 rmsd[a]	χ^2 [b]	nvdw[c]	refinement step 2 rmsd[a]	χ^2 [b]	nvdw[c]
	Structures from FILMAN Run A[d]						
1	Λ-2	0.56	1.33	40	0.45	0.96	44
2	Λ-2	0.53	1.42	55	0.49	0.97	53
3	Λ-2	0.56	1.33	58	0.49	0.97	52
4	Λ-2	0.48	1.38	45	0.45	1.00	37
5	Λ-2	0.56	1.50	39	0.50	0.94	38
6	Λ-2	0.60	1.59	50	0.51	0.98	38
7	Λ-2	0.52	2.09	90	0.47	0.90	34
8	Λ-2	0.60	1.67	48	0.49	0.86	41
9	Λ-2	0.61	2.30	45	0.47	1.01	48
10	Λ-2	0.59	1.84	47	0.52	0.93	42
11	Λ-2	0.58	2.18	54	0.50	1.01	55
	Structures from FILMAN Run B[e]						
12	Δ-1				0.67	6.03	49
13	Δ-1				0.86	6.80	78
14	Δ-3				0.93	2.26	47
15	Δ-3				0.78	3.76	40
16	Δ-3				0.84	3.81	43
17	Δ-3				0.69	4.41	52
18	Δ-4				0.78	4.21	32
19	Δ-4				1.03	4.61	49
20	Δ-5				0.97	4.91	20
21	Λ-3				0.94	7.18	43
22	Λ-8				0.95	4.90	82

[a] Mass weighted best fit of Ga^{3+} and the chelating oxygens to an ideal octahedral coordination sphere with bond distances of 2.0 Å. [b] $\chi^2 = \sum[(d_{obs} - d_{calc})/\text{error}]^2$. [c] Number of van der Waals violations. [d] No configuration constraints were used in the first refinement step. [e] Full set of coordination constraints for each coordination type in both refinement steps.

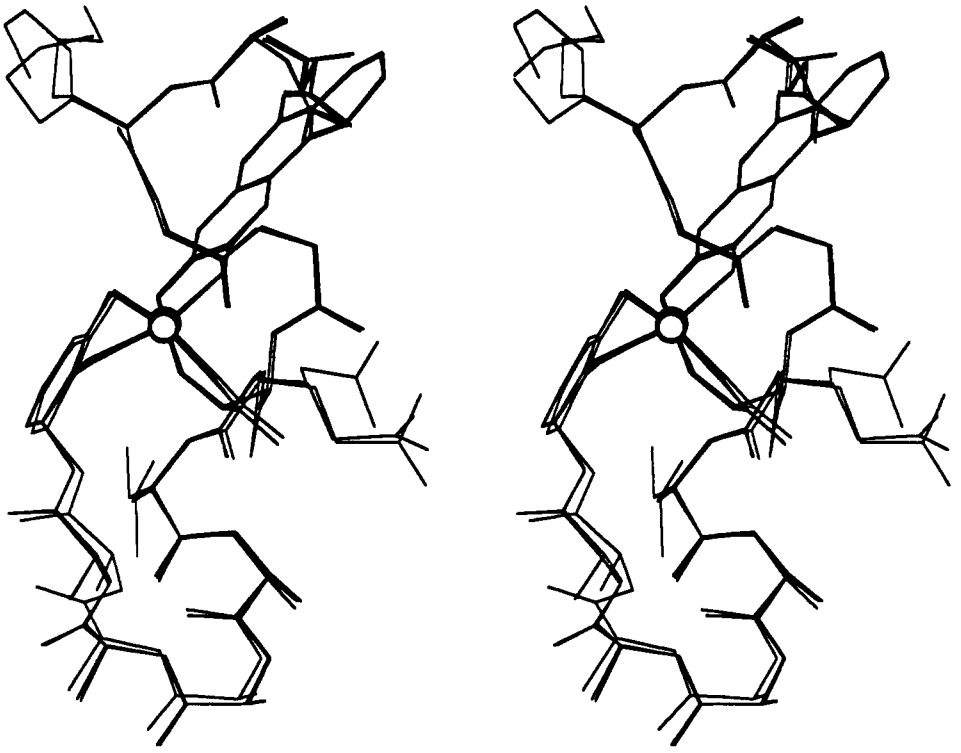

FIGURE 4: Superimposition of the FILMAN structures 1, 6, and 10.

= 2.29×10^{-3} ppm/K, $t_{1/2}$ = 130 min), and Ala^5 ($\Delta\delta/\Delta T$ = 2.29×10^{-3}, $t_{1/2}$ = 360 min) might be involved in intramolecular hydrogen bonds.

The pH dependence of the proton chemical shifts was measured between pH 6.5 and 2.0 (data not shown). Between pH 6.5 and 3.5 no important changes of the spectrum were observed, indicating that probably no structural changes occur in this range. Below pH 3.5 a second component was observed in the spectrum which could be attributed to the free ligand. At pH 2.0 the equilibrium was completely shifted towards the free ligand.

(b) Distance Geometry Calculations. FILMAN is a new method for determination of three-dimensional protein structures from NMR-derived constraints (Koehl et al.,1992), i.e., interproton distances and coupling constants. Dihedral angles are the parameters which are refined during calculation. The method is based on a doubly iterated nonlinear Kalman filter and differs from other methods in directly providing error estimates on the refined parameters. The first iteration step fits the structure to the initial set of distance and dihedral angle constraints. In the second step a van der Waals check is performed. The list of van der Waals violations is used to construct an artificial set of distance constraints which is then treated with the Kalman filter in order to avoid penetration of the van der Waals spheres.

In the first refinement step a set of 33 interproton distance constraints (Table 2) derived from the NOESY spectrum and 10 $^3J_{H\alpha-HN}$ coupling constants was used. The initial variance was always 5% of the constrained distance or coupling constant. For the Ga coordination, eight additional distance constraints between the Ga and the chelating groups taken from the crystal structure of pseudobactin with a very small variance (0.02 Å) were introduced. No constraint between the gallium and the chromophore is necessary because of the construction (see Experimental Procedures). In this set of constraints no information about the absolute configuration of the complex is incorporated.

FILMAN is not able to completely circumvent the local minimum problem (Koehl et al., 1992). Since the final refined structure is somewhat dependant of the starting structure, a set of 200 randomly generated starting structures was considered statistically and refined with FILMAN. The quality of a minimum was judged due to χ^2, the average and maximal error on the initial constraints as well as the number of van der Waals interactions.

The 30 best structures with average errors between 0.6 and 1.1 were examined visually in order to identify the location of the four hydrogen bonds derived from NMR data. The hydrogen bond involving the amide proton of Gly^2 seemed to be a part of a β-turn of type II with the sequence D-Ala-D-Lys-Gly^1-Gly^2. This is confirmed by a strong NOE between Lys-Hα and Gly^1-NH and between the amide protons of Gly^1 and Gly^2. A second β-turn is suggested for the sequence L-Ala^2-D-Ala^3-D-Ala^4-L-Ala^5. The corresponding oxygens of the hydrogen bonds involving (OH)Asp-NH and Ser-NH could not be identified unambiguously at this refinement stage. For each of the identified hydrogen bonds, the H–O distance was constrained to 2 Å. In order to keep the hydrogen bond planar, the distance between the carbon and the nitrogen was constrained to 4.5 Å.

For determination of the absolute configuration of the Ga complex two approaches were chosen. (A) A total of 800 randomly generated starting structures were refined with FILMAN using the initial distance constraint set with additional constraints for the two identified hydrogen bonds. The initial covariance was set to 90° for each dihedral angle. Thirty refinement steps were performed for each starting structure. The result structures were further refined using the same constraints, but with a smaller initial covariance, so that the initial standard deviation for each dihedral angle was 10°.

The 11 best resulting structures were further investigated. The configuration type (Figure 2) was determined by calculating the rmsd between the coordination center (Ga^{3+} and the chelating oxygens) of a given structure and each coor-

Table 4: Mean Dihedral Angles, Standard Deviation (SD), and FILMAN Standard Deviations Extracted from the Final Covariance Matrix of the 11 Structures

	ϕ angle			ψ angle		
residue	average	SD	FILMAN SD	average	SD	FILMAN SD
Chr	−57	–[a]	–[a]	−40	40	10
D-Ala[1]	−51	7	7	−88	101	10
D-Lys	22	19	5	−102	12	17
Gly[1]	−142	14	24	41	7	12
Gly[2]	33	24	12	47	22	9
D-(OH)Asp	78	0.8	3	−3	9	10
D-Gln	−30	22	6	−28	8	7
D-Ser	−67	26	6	−4	28	9
L-Ala[2]	48	45	6	1	173	11
D-Ala[3]	−10	0.9	5	18	5	7
D-Ala[4]	−94	0.8	5	−37	22	11
L-Ala[5]	73	27	9	67	15	13
L-(OH)Orn	−130	10	10	−120	–[a]	–[a]

[a] These angles were not refined in FILMAN calculations.

Table 5: Quality of the Structure

atom 1	atom 2	NMR (Å)[a]	mean (Å)[b]	error (Å)[c]	error (%)	SD[d]	min (Å)[e]
Chr-H1	Ala[1]-HN	2.63	3.45	0.82	31	0.08	3.10
Chr-H10	Lys-HN	4.59	4.72	0.13	3	0.07	4.39
Chr-H10	Gly[2]-HN	3.13	2.98	−0.15	−5	0.13	2.88
Chr-H10	(OH)Asp-HN	3.59	3.93	0.34	9	0.10	3.87
Chr-H10	Gly[2]-HP	3.75	3.20	−0.55	−15	0.00	2.99
Ala[1]-HN	Ala[1]-Hα	2.54	2.25	−0.29	−11	0.00	2.25
Ala[1]-Hα	Lys-HN	2.58	2.46	−0.12	−5	0.24	2.40
Lys-HN	Lys-Hα	2.19	2.57	0.38	17	0.17	2.45
Lys-Hα	Gly[1]-HN	2.21	2.22	0.01	1	0.12	2.15
Gly[1]-HN	Gly[2]-HN	2.85	2.47	−0.38	−13	0.12	2.27
Gly[2]-HN	Gly[2]-Hα	2.43	2.50	0.07	3	0.15	2.42
Gly[2]-HN	(OH)Asp-HN	2.39	3.06	0.67	28	0.00	2.94
Gly[2]-Hα	(OH)Asp-HN	3.23	3.45	0.00	0	0.01	3.20
(OH)Asp-Hα	Gln-HN	3.99	3.28	−0.71	−18	0.04	3.16
(OH)Asp-Hβ	Ser-HN	3.30	3.07	−0.23	−7	0.00	2.90
(OH)Asp-Hβ	Ala[2]-HN	3.38	3.76	0.38	11	0.03	3.56
Gln-HN	Gln-Hα	2.34	2.32	−0.02	−1	0.02	2.31
Gln-HN	Ser-HN	3.14	2.96	−0.18	−6	0.25	2.20
Gln-Hα	Ala[2]-HN	3.93	4.24	0.31	8	0.01	4.11
Ser-HN	Ala[2]-HN	2.91	2.79	−0.12	−4	0.15	2.64
Ser-HN	Ser-Hα	2.30	2.29	−0.01	0	0.00	2.28
Ala[2]-HN	Ala[2]-Hα	2.01	2.36	0.36	18	0.01	2.36
Ala[2]-Hα	Ala[3]-HN	2.27	2.44	0.17	8	0.19	2.18
Ala[3]-HN	Ala[3]-Hα	2.39	2.38	−0.01	0	0.00	2.38
Ala[3]-HN	Ala[4]-HN	3.38	3.15	−0.23	−7	0.03	3.10
Ala[3]-Hα	Ala[4]-HN	3.83	3.45	−0.38	−10	0.04	3.38
Ala[4]-HN	Ala[4]-Hα	2.32	2.32	0.00	0	0.00	2.32
Ala[4]-HN	Ala[5]-HN	2.82	2.26	−0.56	−20	0.03	2.18
Ala[4]-HN	Ala[5]-Hα	3.52	4.37	0.85	24	0.02	4.35
Ala[4]-Hα	Ala[5]-HN	3.52	2.88	−0.64	−18	0.25	2.69
Ala[5]-HN	Ala[5]-Hα	2.15	2.30	0.15	7	0.01	2.30
Ala[5]-Hα	(OH)Orn-HN	2.50	2.53	0.03	1	0.16	2.26
(OH)Orn-HN	(OH)Orn-Hα	2.95	2.95	0.00	0	0.00	2.95

[a] Distance calculated from NOESY spectra. [b] Mean value of the distance in the 11 FILMAN structures. [c] Error = mean (Å) − NMR (Å). [d] Standard deviation of the distances in the 11 FILMAN structures. [e] Minimum distance in the FILMAN structures.

dination type assuming ideal octahedral coordination. The results clearly indicated that all structures belong to the coordination type Λ-2 (Table 3). Only in structures with higher errors other configuration types were found. A further refinement step was performed with 12 additional constraints for the inter-oxygen distances in the coordination sphere to completely fit the structures to octahedral coordination. By inspection of the resulting structures, the two remaining hydrogen bonds were identified. For the amide proton of (OH)Asp a hydrogen bond to one of the chelating oxygens (O1) of the chromophore was found (mean distance, 2.1 Å; mean N–H–O angle, 145°).

(B) In the second approach, the probability of other absolute configurations was investigated. For all possible configurations the O–O distances were calculated by geometrical considerations assuming ideal octahedral coordination and added to the distance constraint list. The variance was set to 0.1 because it was likely that the octahedron was slightly deformed as observed for pseudobactin (Teintze et al., 1981). In this way seven additional constraint sets were constructed, each defining a pair of a Λ configuration and the corresponding Δ-isomer. FILMAN calculations were performed on each constraint set using 200 randomly generated starting structures. Results are shown in Table 3. Minima were found for Δ-1, Δ-3, Δ-4, Δ-5, Λ-3, and Λ-8 configurations with χ^2 values ranging from 2.2 to 7.2 for the configurations cited in Table 3 (run B).

These configurations were found improbable for the following reasons: (i) The structures do not explain the retarded H/D exchange kinetics of the amide protons of (OH)-Asp and Ser because these protons are located at the surface

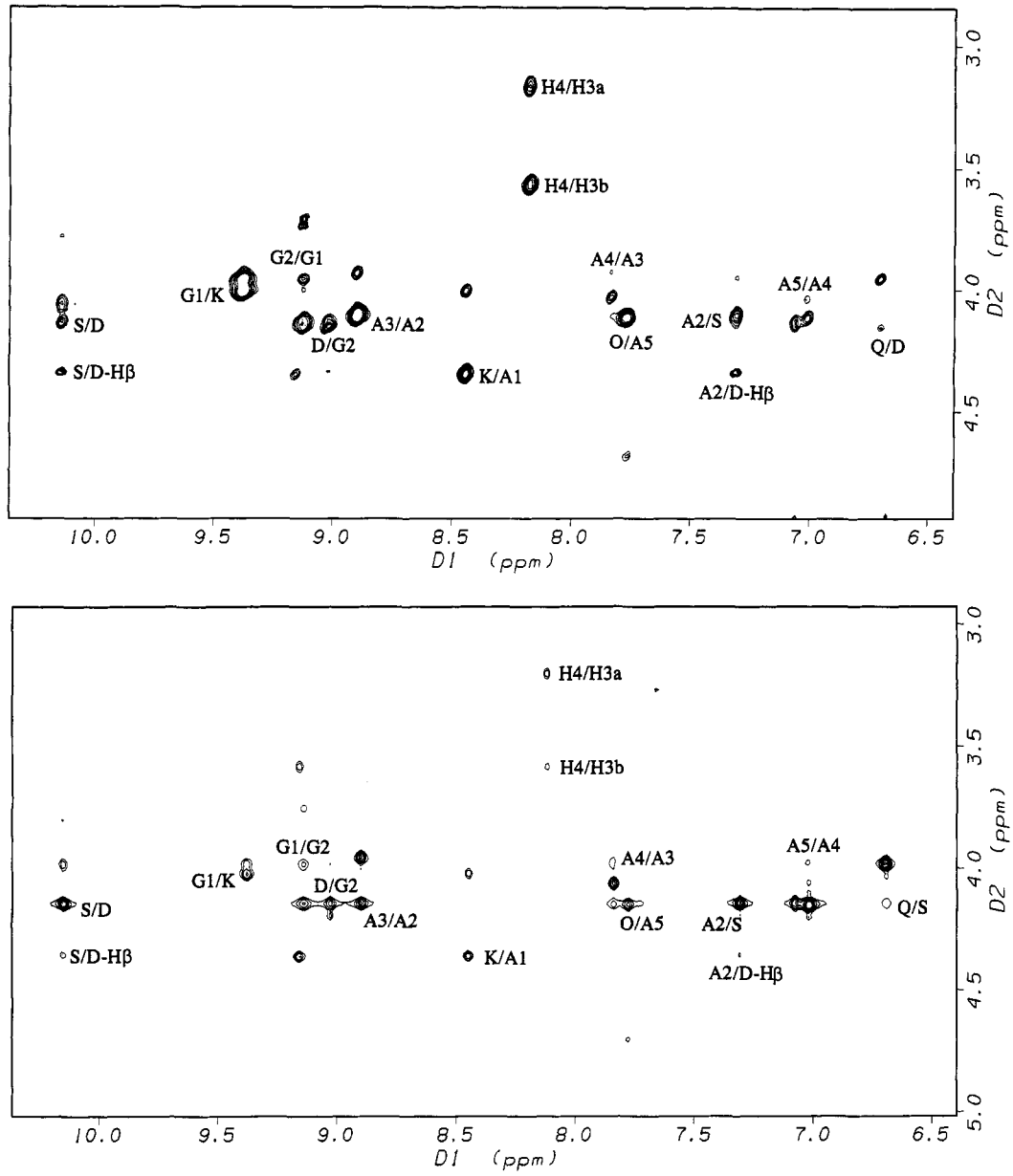

FIGURE 5: (a, top) NH/Hα region of the 500-MHz NOESY spectrum of the Ga(III) complex taken with a mixing time of 200 ms in H_2O/D_2O (95/5, v/v) at pH 4.5, 278 K. (b, bottom) Back-calculated NOESY spectrum of the AMBER structure 4. The overall correlation time was set to 1.2 ns. The line width was 7 Hz and the mixing time 200 ms. Amino acids are named according to IUPAC rules [except D = (OH)Asp and O = (OH)Orn].

of the molecule and are directly accessible to the solvent; (ii) the spectrum back- calculation test (see below) has failed; (iii) the χ^2 values are much higher than those of the Λ-2 configuration. However, the Δ-3 configurations are also in agreement with the experimental results and therefore the coexistence of Δ- and Λ-isomers with an excess of the Λ-isomer could not be excluded rigorously, although it is unlikely.

Comparing the results of the two approaches (A) and (B), one can say that the gallium complex is predominantly Λ-2 configured in aqueous solution.

(c) Quality of the Structure and NOE Back-Calculation. The pairwise mass weighted rmsd calculated for the backbone atom positions of the 11 FILMAN structures was 1.0 Å reflecting the fluctuations in the conformational space which are allowed by the constraint set. A superimposition of three representative structures is shown in Figure 4. The mean dihedral angles and the corresponding standard deviations of the 11 FILMAN structures are given in Table 4. FILMAN standard deviations which are also reported were extracted from the refined covariance matrices. Both standard deviations are generally in the same order of magnitude. A much higher value of the standard deviation calculated over the mean angles is observed for φ and ψ of Ala^2 as well as ψ of Ala^1. This behavior indicates that different values of the dihedral angles are in agreement with the initial constraint set while only slight variations occur during refinement around a local minimum.

The final errors on the experimental data obtained for all interproton constraints are listed in Table 5. Generally, the distances obtained with FILMAN are in agreement with the values derived from NOESY spectra (errors lower than 10%). Some errors are very large because we implied a relatively large initial variance (5% of the constrained distance) on the distance constraints. Positive as well as negative deviations are observed. These errors are explained by the inaccuracy of the experimental data.

Our approach for the determination of interproton distances from the NOESY spectrum involves approximations by

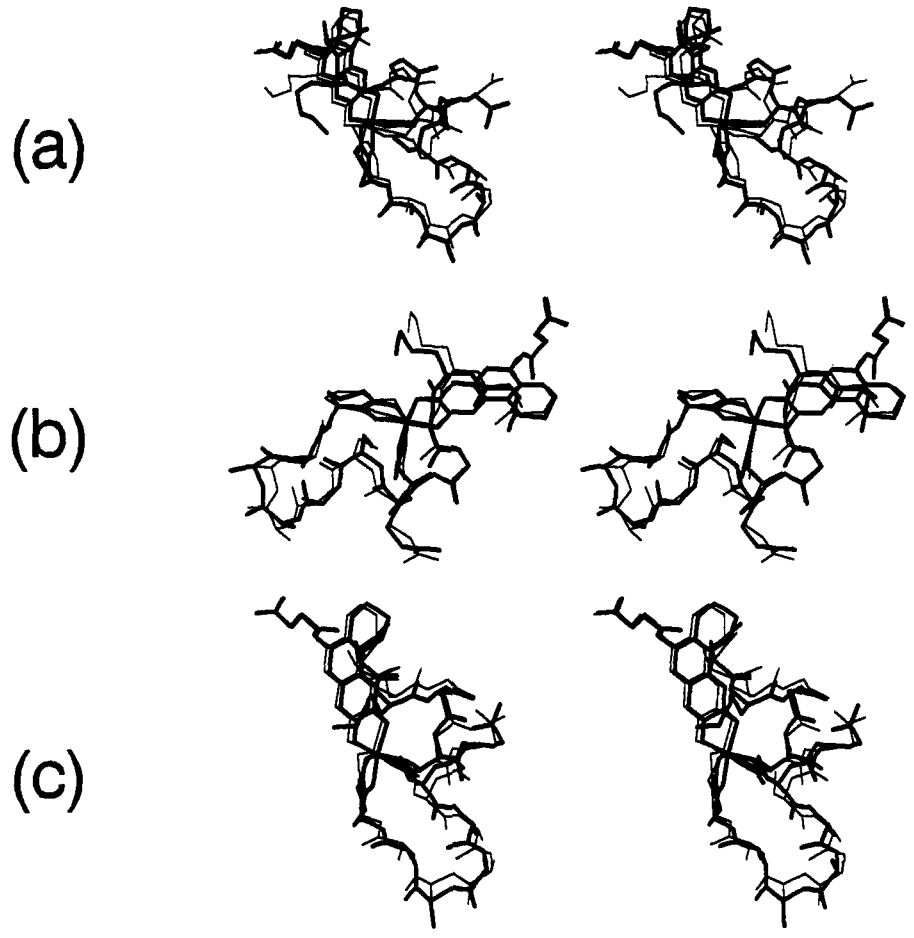

FIGURE 6: Superimposition of representative AMBER structures with the corresponding FILMAN structures from different view points. The AMBER structures are printed with thick lines. (a) Structure 1, (b) structure 4, (c) structure 7.

neglecting: (i) internal motion of parts of the peptide chain, (ii) spin diffusion, and (iii) exchange of the amide protons, so that the calculated distances can be considered as an upper distance limit (Wüthrich, 1986). Therefore, calculated distances which were shorter than those derived from NOESY spectra were not considered as critical. However, six interproton distances were about 20% longer than the experimental values. The error of 31% for the distance between Hα of the chromophore and the amide proton of Ala^1 can be explained by geometrical distortion due to the planar construction of the aliphatic part of the chromophore. This error was easily removed by energy minimization (see below). The error of 28% for the distance between the amide protons of Gly^2 and (OH)Asp is probably caused by an inaccurate integration of the corresponding cross peak, which is very close to the diagonal. However, the remaining large errors [HN-Ala^4/Hα-Ala^5, HN/Hα-Lys, HN/Hα-Ala^2, and Hβ-(OH)Asp/HN-Ala^2] cannot be explained by the reasons cited above. FILMAN calculations with the same constraint set but with a much smaller variance (0.01 Å) for these constraints resulted in the same large deviations from the experimental values, while the overall shape of the resulting structures was not changed.

After each refinement step we calculated a theoretical NOESY spectrum. There was a good agreement of the theoretical and the experimental maps for the 11 Λ-2 structures, while the other configurations could be rejected due to the lack of several cross peaks. Additional cross peaks in the theoretical spectrum were not used as criteria to reject a structure (see discussion above). The regions of the NH/Hα cross peaks of a back-calculated (AMBER structure 4) and an experimental spectrum are compared in Figure 5.

Energy Minimization

Inspection of the 11 Λ-2 structures showed, in addition to the remaining distance errors mentioned above, still important deviations from octahedral configuration as well as up to 55 van der Waals violations. Further refinement of the current structures was performed by restrained energy minimization using the MM2 and the AMBER force field with the interproton constraint set described above. The initial experiments failed due to the lack of suitable parameters for the chromophore and the center of coordination. Therefore, the refinement was performed in two steps: (1) the refinement of the coordination sphere and (2) the refinement of the peptide chain.

The coordination sphere and the chromophore turned out to be well described in the MM2 force field using the parameter set of Allinger (1991) with the extensions described above. Minimization performed on the crystal structure of pseudobactin yielded a mass weighted rmsd over the whole molecule of 0.11 Å. However, MM2 with the current parameter set was not able to handle the peptide chain of the Ga complex of pyoverdin GM-II. Therefore, restrained minimization was performed with strong force constants for the distance constraints (100 kcal/mol·Å^2) and the φ and ψ angles (125 kcal/mol·deg^2) so that the NMR derived constraints were maintained. The van der Waals violations are removed on this stage of refinement while the overall shape of the molecule is maintained.

However, in order to show that our structures were not only kept in the conformation by strong distance and dihedral angle constraints, we performed a further minimization of the peptide chain using the AMBER force field, keeping the chromophore and the chelating groups in the positions calculated with MM2. Interproton distances were the same as used in FILMAN calculations. For distance constraints force constants of 20 kcal/mol·Å^2 were applied, allowing deviations of 0.2–0.3 Å from the constrained values. Most calculations converged rapidly to an energy descent per iteration step of 0.01 kcal/mol. Three representative structures are superimposed to the corresponding FILMAN structures in Figure 6.

DISCUSSION

It was stated in the introduction that the pyoverdins of different *Pseudomonas* spp. and even sub-spp. differ in the composition of their peptidic portions. The sequence of D- and L-amino acids has, therefore, a 2-fold function: It provides the three binding sites for Fe(III) in the correct position, and it is responsible for the recognition of the siderophore at the cell surface. Only the knowledge of the three-dimensional structure of a given pyoverdin allows conclusions regarding the nature and the steric arrangement of the amino acids responsible for an interaction with the receptor site of the outer membrane protein. Inspection of the structure shows that the metal is located on the surface of the molecule and can be set free without large conformational changes, while the polar groups of the peptide chain which may be responsible for the interaction with the receptor are placed on the opposite side of the overall shape. A similar arrangement was found in the crystal structure of pseudobactin where the peptide chain is bent around the Fe(III) forming a circular backbone (Teintze et al., 1981). That the steric arrangement is of importance may be concluded from the observation that one of the chelating units is always at the C-terminal end of the peptide chain or at least close to it (Budzikiewicz, 1993) so that the amino acids responsible for the recognition are part of a more or less rigid structure and not of a free tail. For albomycin, the siderophore of *Streptomyces*, it was shown that, with its help, substances deleterious to the bacterium can be introduced into the cell, which offers a means for a specific attack. The same goal could be envisaged for *Pseudomonas aeruginosa*, a bacterium responsible for serious cases of hospitalism. Due to the complex structures of pyoverdins, it is difficult to modify them chemically in a way that antibiotically active compounds can be attached to them. It may be easier just to handle the part of the molecule which is responsible for the cell-surface recognition. Knowledge of the three-dimensional structure of pyoverdins will help to identify these parts.

REFERENCES

Allinger, N. L. (1977) *J. Am. Chem. Soc. 99*, 8127.

Banks, K. M., Hare, D. R., & Reid, B. R. (1989) *Biochemistry 28*, 6996–7010.

Budzikiewicz, H. (1993) *FEMS Microbiol. Rev. 104*, 209–228.

Cornelis, P., Hohnadel, D., & Meyer, J. M. (1989) *Infect. Immun.* 57, 3491–3497.

Fletcher, R. (1980) in *Practical Methods of Optimization*, John Wiley & Sons, New York.

Gill, P. E., Murray, W., & Wright, M. H. (1981) in *Practical Optimization*, Academic Press, Inc., New York.

Hohnadel, D., & Meyer, J. M. (1988) *J. Bacteriol. 170*, 4865–4873.

Hossain, M. B., Eng-Wilmot, D. L., Loghry, R. A., & van der Helm, D. (1980) *J. Am. Chem. Soc. 102*, 5766–5773.

Karplus, M. (1959) *J. Chem. Phys. 30*, 11–15.

Koehl, P., Lefèvre, J. F., & Jardetzky (1992) *J. Mol. Biol. 223*, 299–315.

Mohn, G., Taraz, K., & Budzikiewicz, H. (1990) *Z. Naturforsch. 45b*, 1437–1450.

Marion, D., & Wüthrich, K. (1983) *Biochem. Biophys. Res. Commun. 113*, 967.

Plateau, P., & Guéron, M. (1982) *J. Am. Chem. Soc. 104*, 7310.

States, D. J., Haberkorn, R. A., & Ruben, D. J. (1982) *J. Magn. Reson. 48*, 286.

Stewart, J. J. P. (1989a) *J. Comput. Chem. 10*, 209.

Stewart, J. J. P. (1989b) *J. Comput. Chem. 10*, 221.

Stewart, J. J. P. (1990) *J. Comput.-Aided Mol. Des. 4*, 1.

Teintze, M., Hossain, M. B., Barnes, C. L., Leong, J., & van der Helm, D. (1981) *Biochemistry 20*, 6446–6457.

van der Helm, D., Baker, J. R., Loghry, R. A., & Ekstrand, J. D. (1981) *Acta Crystallogr. B37*, 323–330.

Weiner, S. J., Kollman, P. A., Case, D. A., Singh, U. C., Ghio, C., Alagona, G., Profeta, S., Jr., & Weiner, P. (1984) *J. Am. Chem. Soc. 106*, 765 –784.

Weiner, S. J., Kollman, P. A., Nguyen, D. T., & Case, D. A. (1986) *J. Comput. Chem. 7*, 230–252.

Wüthrich, K. (1986) in *NMR of Proteins and Nucleic Acids*, Wiley, New York.